

СООБЩЕНИЯ  
ОБЪЕДИНЕННОГО  
ИНСТИТУТА  
ЯДЕРНЫХ  
ИССЛЕДОВАНИЙ

Дубна

95-111

E9-95-111

A.A.Efremov, V.B.Kutner, H.W.Zhao\*, A.V.Lebedev,  
V.N.Loginov, N.Yu.Yazvitskiy

DECRI-14-2, DESIGN ASPECTS  
AND PRELIMINARY RESULTS

---

\*Permanent address: Institute of Modern Physics, Academia Sinica,  
P.O.Box 31, 730000, Lanzhou, China

1995

# 1 Introduction

ECR ion source development at FLNR JINR has been the main ingredient in the upgrading of the U-400M Cyclotron's performance, so-called the project of axial injection beam line. The main idea of building an ECR ion source with good performance in the multiply charged ion production was triggered by the requests of high charge states and high beam intensity for this axial injection beam line. So the new ion source should supply high enough beam intensity with high charge states for heavy elements. Moreover, this new source should be compact with lower electric power consumption and easy to operate for the cyclotron.

The design of the first ECR multicharged ion source DECRIS-14-1 was started at FLNR in 1989 and the first plasma was ignited in January of 1992 [1]. DECRIS-14-1 is MINIMAFIOS type ECR ion source with a large dimension and complicated structure. The electric power consumption of this source is more than 100 KW. The source is very convenient for the investigation of ECRIS properties, but not suitable to be coupled to U-400M cyclotron.

In such background, the second ECR ion source DECRIS-14-2 was proposed in the middle of 1992. The physical and technical design of this new source was finished in the beginning of 1993. The first plasma was ignited in November of 1994. The preliminary test and optimization for highly charged ion production have been performed since December of 1994. Now DECRIS-14-2 is ready to be put into operation for the U-400M cyclotron.

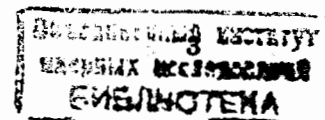
## 2 Source Structure and Magnetic Field Configuration

Figure.1 illustrates the source structure. The main parameters are listed in Table .1 .

This source shares many common features with that of CAPRICE source [2] and GANIL ECR4 [3] , such as , plasma chamber with a double wall so that cooling water could be running around to avoid

Table 1. Main Parameters of the DECRIS-14-2

<u>AXIAL MAGNETIC FIELD</u>	
Peak on axis	1.2 T
Typical solenoid current	950 A
Maximum solenoid current	1000 A
Length of the second stage mirror	19 cm
<u>HEXAPOLE</u>	
External diameter	19. cm
Internal diameter	7. cm
Hexapole length	20. cm
Hexapole field on chamber wall	1.1 T
<u>PLASMA CHAMBER</u>	
Internal diameter for second stage	6.5 cm
Internal diameter for first stage	2.9 cm
Length for the second stage	22. cm
<u>SOLENOID</u>	
Solenoid number	2
Internal diameter	18. cm
External diameter	34. cm
Pancake number	6 Double pancake
Number of the layers	9
Maximum electric power consumption	60 Kw
Cooling water flow rate	27. l/min
Cooling water pressure	5 atm
Length of the wire for two solenoids	170 m



corrosion problems due to cooling, so the cooling liquid is never in contact with the FeNdB permanent magnet; the copper coaxial line for the rf power coupling and gas feeding, also possible for solid ion production with a micro-oven or insert rod in it; the cone-shape ring around the first stage used for raising the axial magnetic field peak and defining the peak position; the two solenoids for the production of axial mirror magnetic field; the iron yoke around the coils for increasing the axial field at each end; the iron ring between the two solenoids dedicated to the reduction of the axial field in the center to achieve a required mirror ratio. The plasma chamber and hexapole are insulated from the solenoids and the main vacuum pumps.

Each of the magnetic solenoids shown in Fig.1 consists of 6 double pancakes. Each pancake has 9 turn layers of 5.0 mm hollow-core copper wire. The two solenoids are placed around the extremities of the hexapole and totally embedded in an iron yoke. The axial magnetic field distribution is shown in Fig.2 from which we can see the calculated distribution is in a very good agreement with the experimental measurement. The axial magnetic mirror is inside the length of the hexapole. The peak of axial mirror magnetic field at the injection side is as high as 1.2 T. The gradient of the magnetic field along the radius and the axis is also very high from 0.4 T to 1.2 T which is supposed to be beneficial to the multiply charged ion production. The amplitude of the axial field at the extraction side is relatively small up to 0.85 T.

In order to minimize the magnetized volume and leave more space to the coils, the hexapole with a special structure consists of three parts with different external diameter. The central part of the hexapole has a large thickness to get an intensive radial field on the wall so as to enhance the plasma confinement, since the main ECR plasma is situated in the central region of the chamber. The two extremities of the hexapole can be smaller because the axial magnetic field is maximum. So it is possible to use small diameter coils where the axial field must be maximum. The central part of the hexapole is made up of 24 pieces on the base of the Halbach construction, 7.0 cm in internal diameter, 19 cm in external diameter and 10 cm in length. The cross section is shown in Fig.3. The calculated magnetic field along

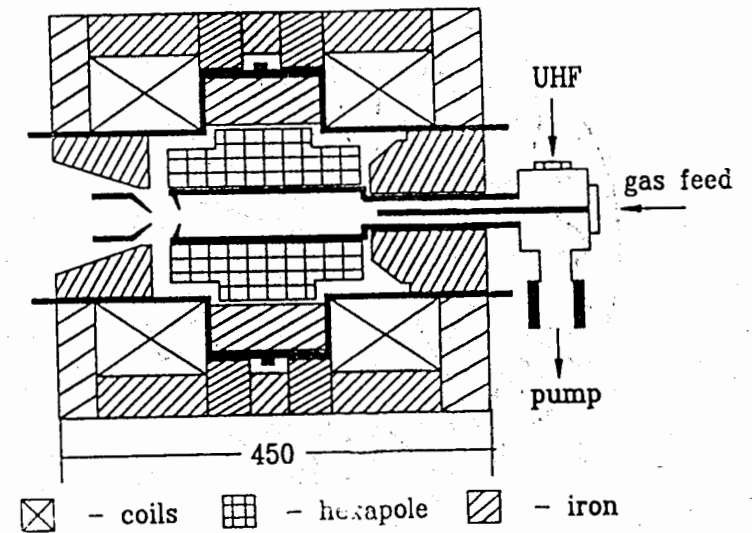


Fig.1 Schematic form of DECRIS-14-2

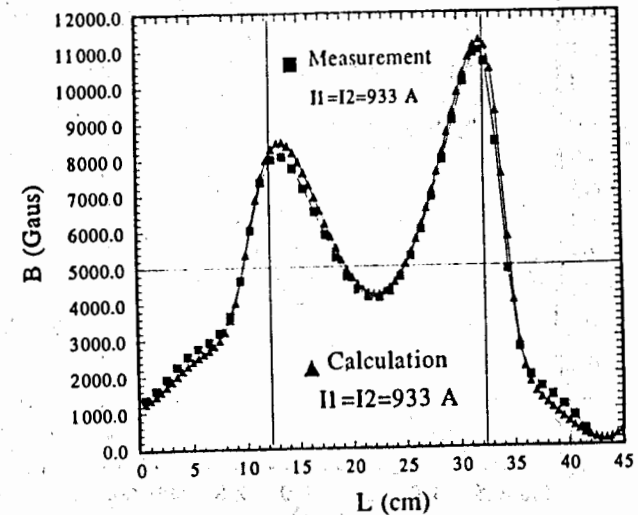


Fig.2 Axial magnetic field distribution

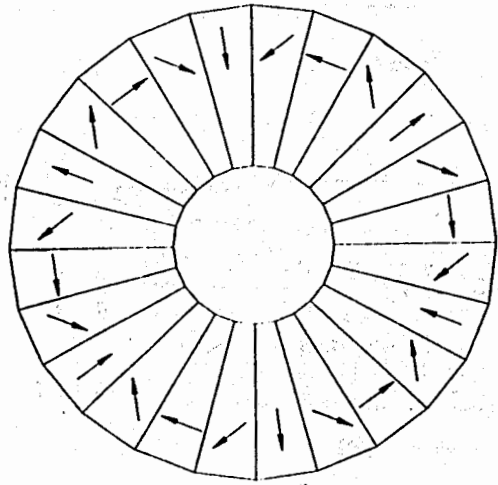


Fig.3 The cross section of the hexapole at the central part

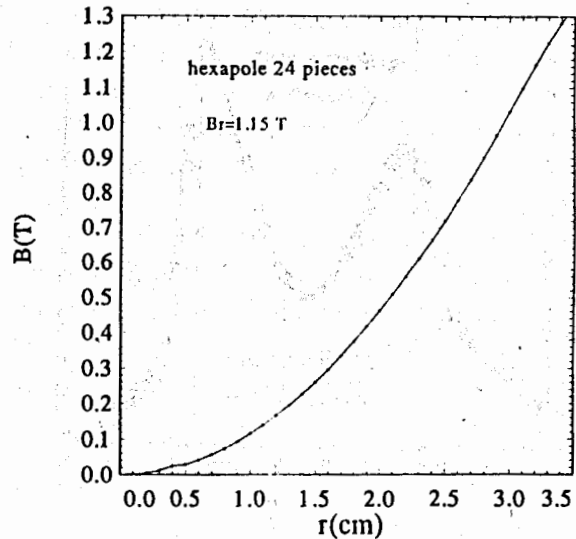


Fig.4 Calculated radial magnetic field of the hexapole at the central part ( 24 pieces )

the radius is demonstrated in Fig.4. In every segment the easy axis orientation keeps in the same direction, and the easy axis orientation advances by 60 degree from one segment to the next. The extremities of the hexapole are similar to the central part, but made up of 12 pieces, 7.0 cm in internal diameter, 17 cm in external diameter and 5 cm in length respectively. The easy axis orientation advances by 120 degree from one segment to the next. The radial magnetic field of the whole hexapole was measured , as shown in Fig.5. We can see the field distribution at the central part along the axis is quite uniform which is important for an ECR ion source. On the wall ( $r \sim 32mm$ ) the field can reach more than 1.1 T. The radial magnetic field distribution in athimthal direction was also measured at the center of the hexapole with different radius, as it is shown in Fig.6.

The extraction system of the source consists of a plasma electrode with 8 mm exit hole and a stainless steel puller with 12 mm hole, the distance between them is about 30 mm. The plasma electrode is situated near the extraction peak of the axial magnetic field. The optimum position of the plasma electrode should be determined experimentally.

### 3 Preliminary Results to Gaseous Elements and Optimization to Highly Charged Ion Production

The source has been tested with nitrogen , oxygen, neon, argon and xenon. The highly charged ion production of these gases has been optimized by the gas mixing effect and a negatively biased electrode (no first stage).

In the gas mixing, main gas and support gas are fed by two separated piezoelectric valves located near the first stage. The mixture of main gas and support gas is feeding into the source through the coaxial line. It is also possible to feed the support gas from another port near the first pump.

In the design of the negatively biased electrode, considering the simplicity, the negatively biased potential is applied directly to the

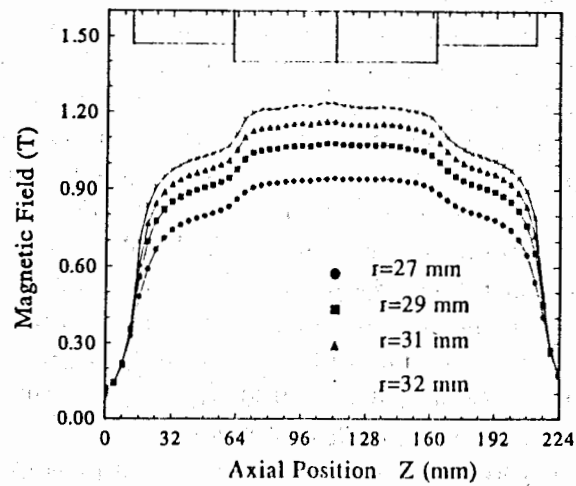


Fig.5 The measured radial magnetic field of the hexapole along the axis at different radius.

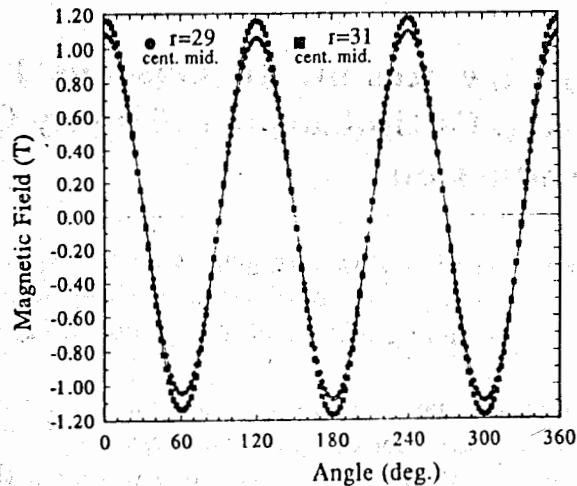


Fig.6 The measured radial magnetic field distribution in azimuthal direction at the center of the hexapole

coaxial line which is insulated from the other part of the source with the high voltage, in this case, We should try to prevent the microwave passing through the insulator between the coaxial line and the copper cube in order to avoid microwave leakage and the heating to the copper cube. The position of the negatively biased electrode is important and should be optimized. We put it at the peak of the axial magnetic field.

The preliminary results are summarized in Table 2. The typical spectrums for oxygen and argon are shown in Fig.7 and Fig.8.

By means of the negatively biased electrode and the gas mixing effect, the typical ion currents with high charge states are improved averagely by 2.3 times compared with using the traditional compact first stage. The typical ions that we optimized are  $O_{16}^{6+}$ ,  $Ar_{40}^{11+}$  and  $Xe_{132}^{18+}$ . In Fig.9 we present the comparison between the results with the first stage and the results optimized by the negatively biased electrode and the gas mixing for the highly charged ions of oxygen, argon and xenon. The currents and enhancement factors of the typically optimized ions by the negatively biased electrode and the gas mixing effect are listed in Table 3. The comparison of the typical ion currents with the first stage and the negatively biased electrode (no first stage) is given in Table 4 (in both cases with the gas mixing effect). Compared with the traditional compact first stage (with a quartz tube), we can see from Table 4 that the negatively biased electrode (no first stage) increases the currents of highly charged ions averagely by 1.5 factor when the gas mixing effect exist in both cases.

When we tuned the source, the ion currents keep rising with increasing the negatively biased potential, and then saturate. Fig.10 shows the dependence of the ion current on the negatively biased potential when we optimized  $Ar^{9+}$ . The negatively biased potential has to be optimized according to different ions, axial magnetic field, rf power and gas feeding rate. The optimized negatively biased potential increase with the coupled rf power and the mass of the optimized ion, as shown in Fig.11 and Fig.12. When the negatively biased potential is increased, the gas feeding rate usually has to be decreased.

We also tested the first stage together with the negatively biased potential when we optimized  $Ar^{9+}$ . The enhancement factor by the negatively biased potential together with the first stage is much less

Table 2. The Preliminary Results from DECRIS-14-2 ( $\mu A$ )

I \ Q	5	6	7	8	9	10	11	12	13	14	15	16	17	18	19	20
$N_{14}$	110	20														
$O_{16}$	180	135	24													
$Ne_{20}$		90	56	20												
$Ar_{40}$				166	98	25										
$Xe_{132}$								20	23	26		29	31	28	18	

\*: All the currents were got with rf power less than 250 W and extraction voltage 10 KV.

Table 3 The currents and enhancement factors of the typically optimized ions by the negatively biased electrode and the gas mixing effect.

I ( $\mu A$ )	First Stage	Negatively Biased Electrode + Gas Mixing Effect	f
$O_{16}^{6+}$	60	135	2.25
$Ar_{40}^{11+}$	11	25	2.27
$Xe_{132}^{18+}$	14	31	2.21

Table 4. Comparison of the typical ion currents from DECRIS-14-2 with the first stage and the negatively biased electrode

I ( $\mu A$ )	First Stage	Negatively Biased Electrode	Enhancement Factor
$O_{16}^{6+}$	90	135	1.5
$Ar_{40}^{9+}$	63	98	1.56
$Ar_{40}^{11+}$	16.5	25	1.52
$Xe_{132}^{18+}$	23	31	1.35
$Xe_{132}^{19+}$	22	28	1.27

\*: In both cases with the gas mixing.

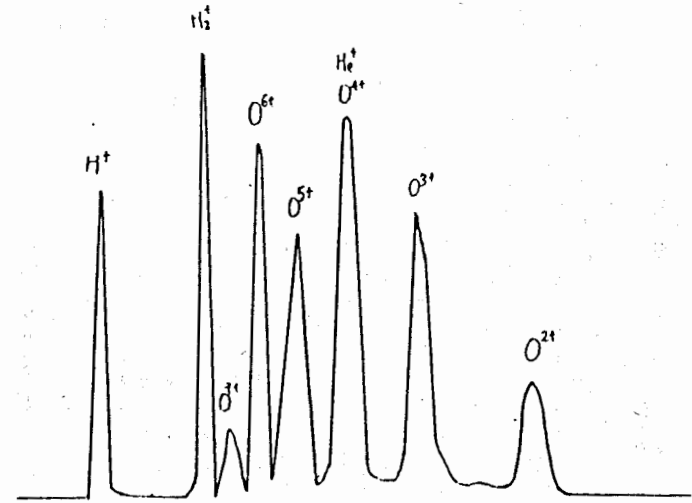


Fig.7 Oxygen spectrum optimizing for  $O^{6+}$

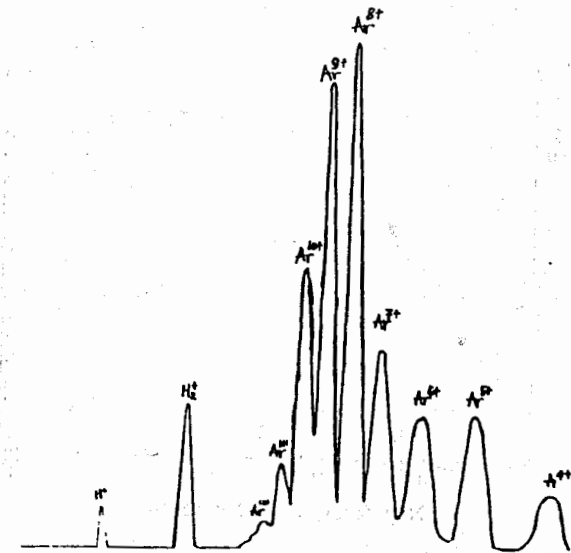


Fig.8 Argon spectrum optimizing for  $Ar^{11+}$

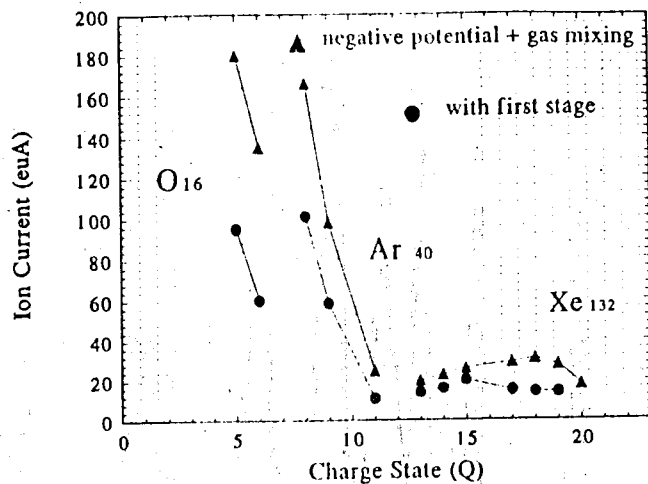


Fig.9 Comparison between the results with the first stage and the results optimized by the negatively biased electrode and the gas mixing effect for the highly charged ions of oxygen, argon and xenon.

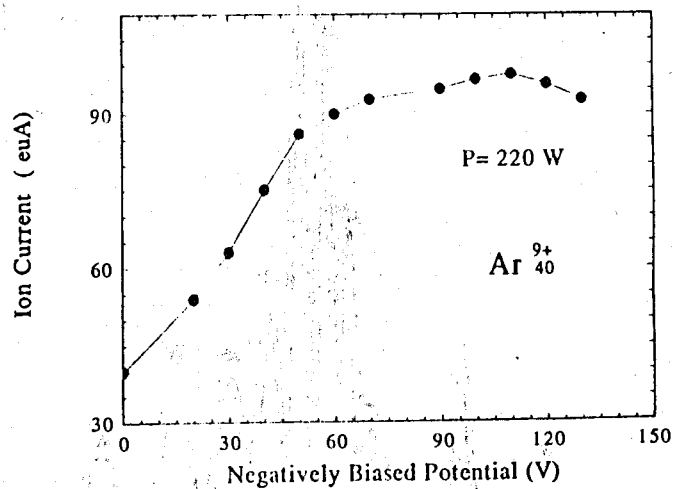


Fig.10 Dependence of the ion current ( $Ar_{9+}$ ) on the negatively biased potential.

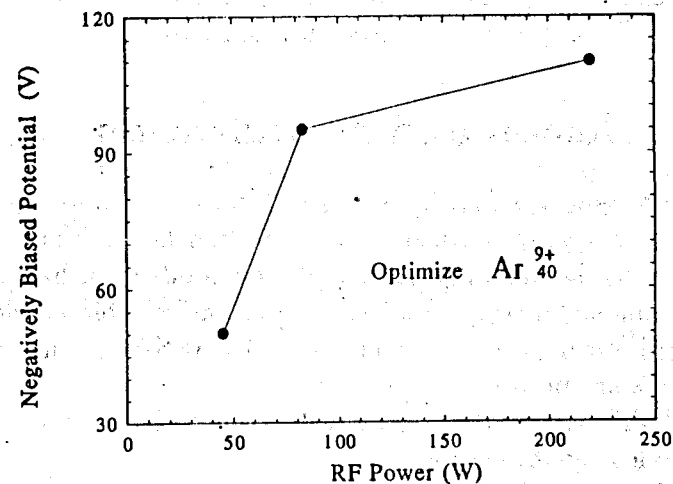


Fig.11 The optimized negatively biased potential versus the coupled rf power.

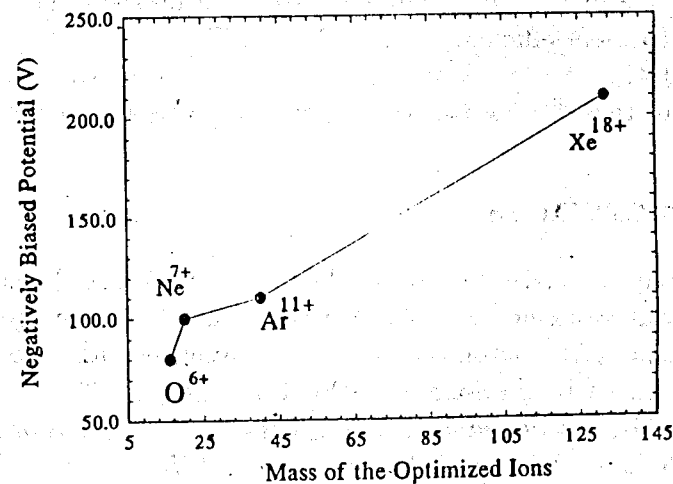


Fig.12 The optimized negatively biased potential versus the mass of the optimized ion.

than the negatively biased electrode without the first stage. The ion current of  $Ar^{9+}$  only increases from  $60 \mu A$  to  $76 \mu A$ .

## 4 Conclusion and Modification

The preliminary test of DECRIS-14-2 to the gaseous multiply charged ion production was performed. The operation and performance are stable and reliable. The highly charged ion production has been optimized by the gas mixing effect and the negatively biased electrode. In order to improve the performance of DECRIS-14-2, the following modifications are planned:

(1). Modification to the negatively biased electrode in order to prevent the leakage of microwave power.

(2). Add the cooling system to the part of rf power coupling so that we could increase rf power more than 400 W.

(3). Put two slits with adjustable-width in the front of and after the analyzing magnet to improve the resolution; re-calculation of the optics for the beam line of our test bench to improve the transport efficiency (present efficiency is less than 30 %).

(4). Optimize the position and the exit hole size of the plasma electrode to raise the extraction of the highly charged ions.

## 5 References

- [1]. A.Efremov, V.Kutner, A.N.Lebedev, et al, Proceedings of 11th International Workshop on ECR Ion Sources, 1993, Groningen, P.159
- [2]. B.Jacquot, M.Pontonier, et al, Proceedings of 10th International Workshop on ECR Ion Sources, 1990, Tennessee, P.133
- [3]. P.Sortais, P.Aital, et al, Proceedings of 10th International Workshop on ECR Ion Sources, 1990, Tennessee, P.35

Received by Publishing Department  
on March 17, 1995.